T1 and T2* responses to hypercapnic and hyperoxic gases in normal tissue are independent of the order of gas delivery

J. D. Winter[1,2], M. Estrada[1], and H-L. M. Cheng[1,3]
[1]Physiology and Experimental Medicine, The Hospital for Sick Children, Toronto, Ontario, Canada, [2]Research and Development, IMRIS, Winnipeg, Manitoba, Canada, [3]Medical Biophysics, University of Toronto, Toronto, Ontario, Canada

Introduction: Quantitative MRI measures of T_1 and T_2* relaxation times offer a noninvasive means to indirectly monitor tissue O_2 content. T_1 oxygen-dependence is primarily based on the presence of weakly paramagnetic molecular O_2 dissolved in blood plasma and interstitial space; whereas, T_2* oxygen dependence is based on the signal loss induced by local magnetic field inhomogeneities generated by paramagnetic deoxy-hemoglobin. The clinical rationale for gas challenge studies originate from radiotherapy strategies aimed at augmenting tissue oxygenation via increased fraction of inspired O_2 (FiO_2) and/or CO_2 ($FiCO_2$). Inclusion of CO_2 in the inhaled O_2 gas mixture was proposed to reduce O_2-induced blood flow reductions, and previous studies have demonstrated differential T_1 and T_2* responses to breathing carbogen and 100% O_2[1,2]. However, in these studies the underlying tissue oxygenation and perfusion status were not investigated, and gases were delivered in a fixed order. The objective for the current study was to characterize T_1 and T_2* responses to various combinations of FiO_2 and $FiCO_2$ in rabbit abdominal tissues. Potential blood flow and partial pressure of O_2 (pO_2) dependence on previous gas challenges were examined by randomizing the gas challenge order in each subject. Following the imaging sessions, pilot measurements of tissue pO_2 and perfusion were conducted to assess temporal dynamics that may contribute to MR relaxation time changes.

Methods: All animal studies were approved by our institutional animal care committee. Quantitative T_1 and T_2* MRI parameters were collected from five New Zealand white rabbits (4.0 - 4.5 kg) in six imaging sessions with various combinations of FiO_2 and $FiCO_2$. Each rabbit was induced with 5 % isoflurane, and maintained at 1 % for the MR experiments and 2 % for the invasive studies. The following gas challenges were delivered in random in 5 - 8 different steps: room air (21% O_2, balanced N_2), 10% CO_2 (balanced air), 100% O_2, and carbogen (10% CO_2 and 90% O_2). MR imaging was performed on 1.5 T GE scanner (Signa EXCITE TwinSpeed; General Electric Healthcare, Milwaukee, WI, USA) using a transmit/receive quadrature knee coil, with coronal images slices positioned to encompass the kidney, liver, and paraspinal muscle. T_1 quantification was achieved using a variable flip angle approach, with a series of 3D fast spoiled gradient recalled echo scans with the following imaging parameters: TR = 7.2 ms, TE = 3.1 ms, FA = 2, 10 and 21°, FOV = 160 mm, matrix = 256 × 160, slice thickness (SL_{TH}) = 3 mm, number of slices (N_{SL}) = 10, N_{AVG} = 4. T_2* quantification was achieved using a 2D multi-echo gradient-echo sequence with the following parameters: TR = 100 ms, 16 equally spaced TEs = [2.1 – 47.1] ms, FA = 30°, FOV = 160 mm, matrix = 256 × 192, SL_{TH} = 3 mm, N_{SL} = 6, and N_{AVG} = 4. Pixel-wise T_1 and T_2* maps were generated using in-house Matlab (V.7.0, Mathworks Inc., Natick, MA, USA) scripts. T_1 parameter maps were generated using the signal equation for the SPGR steady state magnetization with analytical-based flip angle correction using B_1 field maps acquired separately[3]. T_2* parameter maps were computed by fitting T_2* signal intensity versus echo time to a monoexponential signal decay function[4]. Regions-of-interest were outlined in the liver, kidney and muscle to extract mean T_1 and T_2* values for each gas challenge.

Invasive tissue measurements were conducted in a separate session with OxyLite and OxyFlo (Oxford Optronics, Oxford, UK) fibre optic probes that were inserted into the three tissue types (liver, kidney, and muscle). The OxyLite uses fluorescence lifetime measurements to quantify absolute tissue pO_2 and OxyFlo uses laser Doppler to provide relative measures of tissue perfusion.

Relative ΔT_1 and ΔT_2* values were computed for each transition between the different gas challenges, and a series of one-tailed one-sample t-tests were performed to determine significant differences from zero (null hypothesis).

Results: Figure 1 provides the ΔT_1 and ΔT_2* values for each of the transitions from air to one of the three inspired gas challenges. All transitions exhibited expected trends, especially in liver and kidney. Key observations include trends toward positive ΔT_2* for air → 100% O_2, negative ΔT_2* on air → 10% CO_2, and equivocal ΔT_2* on air → carbogen. Significance for ΔT_2* transitions existed for air → 10% CO_2 in liver ($p < 0.01$) and air → 100% O_2 in kidney ($p < 0.05$). Muscle ΔT_2* were very small and insignificant, and air → carbogen transitions produced inconsistent ΔT_2* in all tissues. ΔT_1 values exhibited variability, with only kidney air → 100% O_2 ($p < 0.05$) transition exhibiting significance. Figure 2 provides ΔT_1 and ΔT_2* for transitions between the three different gas challenges. Expected trends were also observed: positive ΔT_2* and negative ΔT_1 on 10% CO_2 → 100% O_2/carbogen, and reverse changes for 100% O_2→ carbogen. ΔT_2* significance was achieved in both liver and kidney on all transitions: 10% CO_2 → 100% O_2/carbogen ($p < 0.05$) and 100% O_2 → carbogen ($p < 0.01$). For muscle, only the negative ΔT_2* for 100% O_2→ carbogen ($p < 0.05$) was significant. ΔT_1 did not reach statistical significance for any gas transitions, except muscle transitions from 10% CO_2 → 100% O_2 and 100% O_2 → carbogen ($p < 0.05$).

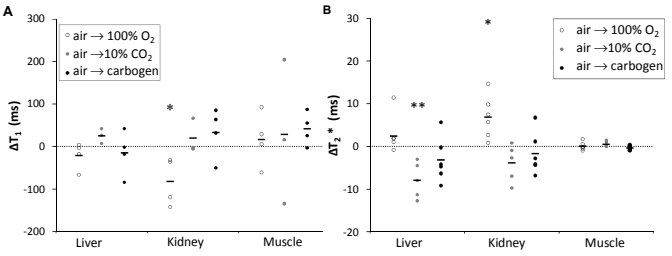

Figure 1. ΔT_1 (a) and ΔT_2* (b) values for each gas transition from air in three tissues. * $p < 0.05$, ** $p < 0.01$

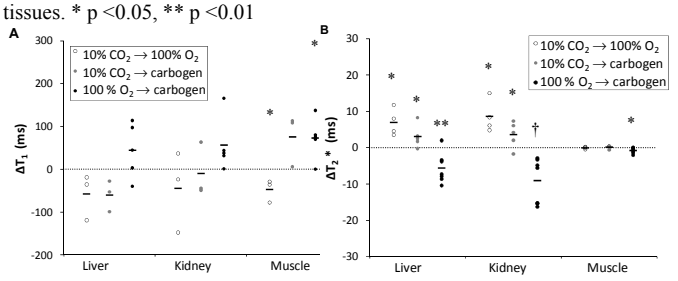

Figure 2. ΔT_1 (a) and ΔT_2* (b) values for transitions between gas challenges in three tissue types. * $p < 0.05$, ** $p < 0.01$, † $p < 0.005$

Figure 3 provides a representative OxyFlo tissue pO_2 and OxyLite perfusion time series in the liver. The invasive measurements demonstrated consistent trends in tissue perfusion and oxygenation changes but considerable variability in their absolute values and temporal dynamics.

Discussion: Although the principle clinical application for MR-based oxygenation monitoring is in oncology, there is still much to learn from normal tissue changes. In this study, we found that T_2* changes followed predicted patterns: ↑ T_2* on 100% O_2 (due to higher pO_2) and ↓ T_2* on 10% CO_2 (due to higher Hb and blood volume). Similarly, T_1 changes followed predicted trends toward a ↓ T_1 on 100% O_2 (due to higher pO_2 and lower blood volume) and ↑T_1 on 10% CO_2 (due to greater blood volume). However, T_1 changes were much less predictable, compared with T_2*. The air → carbogen transition generated the most variable T_1 and T_2* transitions, possibly attributed to opposing influences from observed perfusion and pO_2 changes. A previous study in normal human abdominal tissues found results which are inconsistent with the T_1 and T_2* transitions in our study[1]. This cited study reported T_1 decreases and non-significant T_2* changes for air → 100% O_2 and T_1 increases and T_2* decreases for air → carbogen[1]. This distinction suggests physiological differences between the two studies may exist. For the invasive measures, we found large variability in the temporal dynamics of tissue perfusion and pO_2, which is a consideration for future studies. In conclusion, we found that T_2* provided greater sensitivity to changes in tissue pO_2 and perfusion compared with T_1, and we also found independence of relaxation time changes from order of gas administration. Variability in our study and the literature may be partly attributed to organ-specific pO_2 and perfusion dynamics exhibited in this study.

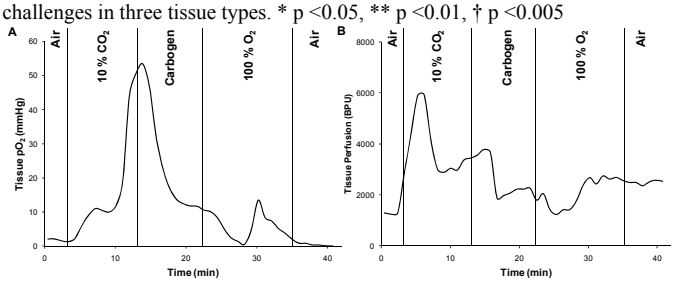

Figure 3. Representative OxyLite pO_2 values (a) and OxyFlo relative perfusion measurements (b) in the rabbit liver.

References: 1. O'Connor JP *et al.*, Magn Reson Med 2009,**61**:75-83; 2. O'Connor JP *et al.* Magn Reson Med 2007,**58**:490-496; 3. Cheng HL *et al.*, Magn Reson Med 2006,**55**:566-574; 4. Beaumont M, *et al.*, J Magn Reson Imaging 2009,**30**:313-320.